Inorganic Chemistry

Article

pubs.acs.org/IC

Phosphorus(V)-Corrole: Synthesis, Spectroscopic Properties, Theoretical Calculations, and Potential Utility for *in Vivo* Applications in Living Cells

Xu Liang,[†,‡] John Mack,[†,§] Li-Min Zheng,[‡] Zhen Shen,[‡] and Nagao Kobayashi*[,†]

[†]Department of Chemistry, Graduate School of Science, Tohoku University, Sendai 980-8578, Japan

[‡]State Key Laboratory of Coordination Chemistry, Nanjing University, Nanjing 210093, People's Republic of China

[§]Department of Chemistry, Rhodes University, Grahamstown 6140, South Africa

Supporting Information

ABSTRACT: The synthesis and properties of phosphorus(V) 5,10,15-tris(4-methoxycarbonylphenyl)corrole (**1**) have been investigated, and its potential utility for bioimaging applications in living cells has been explored. As would normally be anticipated for corrole complexes, the intensity of the Q(0,0) bands of **1** is greater than those of comparable phosphorus(V) tetraphenylporphyrins, but the Φ_F values (0.25 for **1**) are found to be comparable. A detailed analysis of the electronic structure of the complex was carried out by comparing electronic absorption and MCD spectral data to the results of TD-DFT calculations. The *meso*-aryl substituents, which enhance the lipophilicity of **1** and hence result in its localization in intracellular membranes during HeLa cell experiments, are predicted to result in a narrowing of the HOMO−LUMO gap and hence a red shift of the Q(0,0) bands toward the optical window in biological tissues.

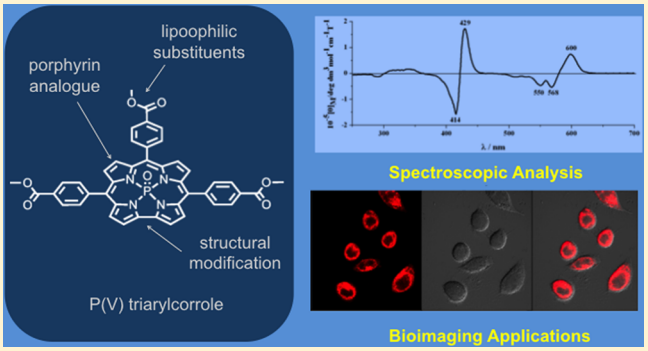

INTRODUCTION

The porphyrinoid complexes of nonmetals have received a considerable amount of attention in recent years, since their optical and biological properties could lead to applications as functional dyes in a number of different high-technology fields, such as organic solar cells, photodynamic therapy, heat absorbers, and organic catalysis.[1] Porphyrins tend to have high fluorescence quantum yields due to their rigid planar structures and emission bands that lie at the red end of the visible region in the optical window in biological tissues between 650 and 1000 nm, making them potentially suitable for bioimaging applications.[2] Ideally a bioimaging dye molecule should absorb and emit strongly in the red/near-infrared (NIR) spectral region with narrow spectra bands, large Stokes shifts, long excited-state lifetimes, excellent photostability, and low biotoxicity. The main disadvantage of porphyrins in this regard is that their lowest energy $\pi \rightarrow \pi^*$ band (usually referred to as the Q band) tends to be relatively weak with molar extinction coefficients of $>10^4$ L mol^{-1} cm^{-1},[3] so the bioimaging properties of structural analogues such as chlorins,[4] which absorb more strongly at the red end of the visible region, have also been studied.

Corroles are porphyrin analogues with a direct pyrrole−pyrrole bond and an extra NH proton on the inner ligand perimeter, best known for forming the basic structure in vitamin B_{12}.[5] In recent decades, there has been a strong research focus on the use of corroles as functional ligands, largely due to their ability to stabilize higher oxidation states of the coordinated metal such as Cr(V), Fe(IV), Co(IV), and even Mn(V) or Co(V).[6] Although much of the research has focused on the complexes of first-row transition metal ions,[7] which tend to be nonfluorescent due to the presence of low-lying charge transfer states associated with the central metal, the potential utility of sulfonated Ga(III) corroles for combined photodynamic therapy and bioimaging applications in living cells has recently been explored.[8] There has been comparatively little research on the corrole complexes of other main group ions relative to the porphyrins due primarily to difficulties faced in their syntheses and isolation.[7,9] P(V) corrole complexes have been prepared by reacting metal-free corroles with a P(V) reagent.[7,10] There is an intensification of the Q band relative to those of analogous P(V) porphyrins,[11] and it lies at similar wavelength to those of P(V) tetraphenylporphyrins between 590 and 610 nm.[11c] Phosphous(V) porphyrins have been reported to have low biological toxicity, and satisfactory results have been reported in biological systems for the photosensitized formation of singlet oxygen.[12] It seems reasonable to anticipate that structural analogues such as corroles will have similar properties in this regard.

Received: September 17, 2013
Published: March 5, 2014

   dx.doi.org/10.1021/ic402347w | *Inorg. Chem.* 2014, 53, 2797−2802

Scheme 1. Synthetic Procedure for the Formation of the P(V) 5,10,15-Tris(4-methoxycarbonylphenyl)corrole Derivative (1)

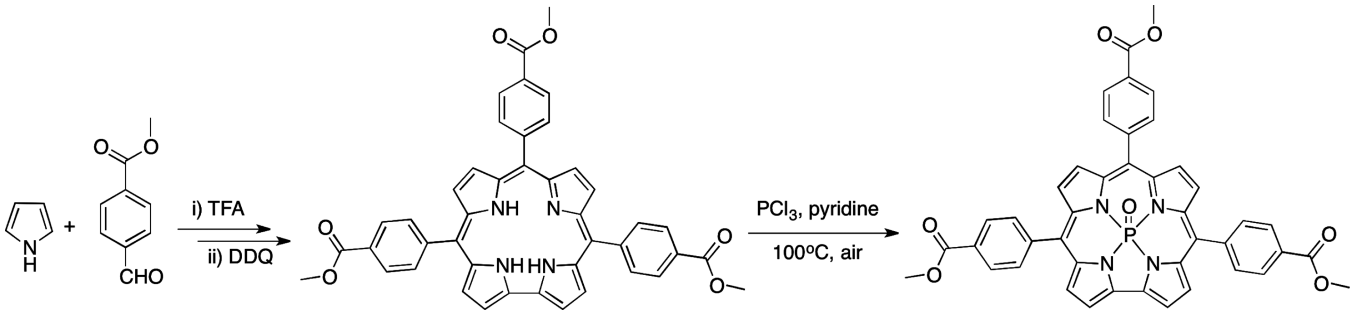

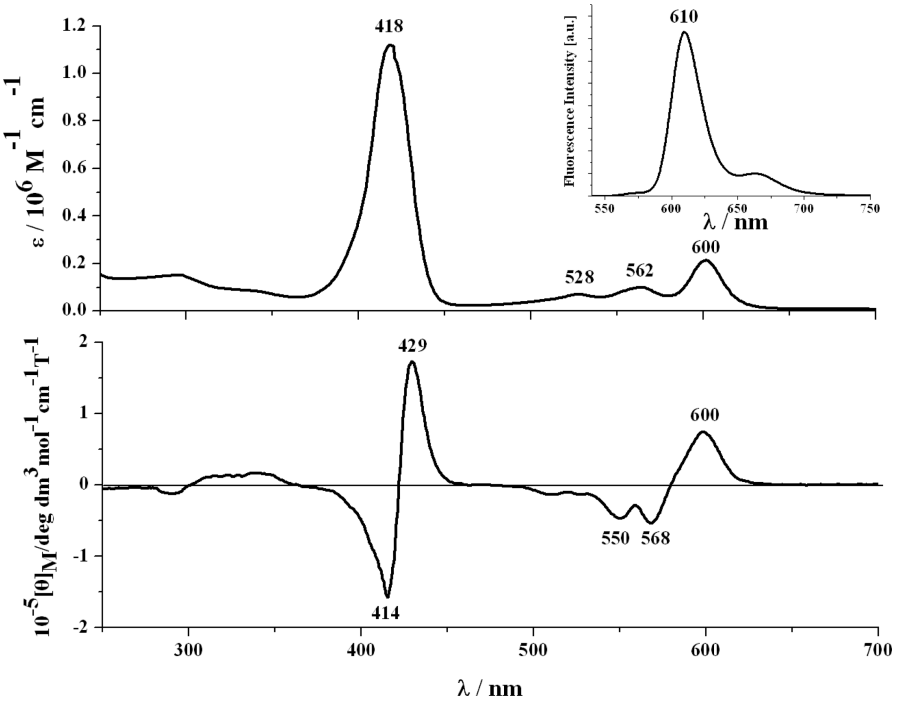

Figure 1. UV−visible absorption and MCD spectra of **1**, with the fluorescence intensity in the Q band intensity provided as an inset.

In this paper a novel P(V) 5,10,15-tris(4-methoxycarbonylphenyl)corrole has been prepared to study trends in the electronic structure and spectroscopic properties of P(V) corrole complexes and their potential utility for bioimaging applications in living cells. The ester groups on the *meso*-substituents were expected to enhance the lipophilicity and hence enhance cellular uptake, since a lipophilic 4,4-difluoro-4-bora-3a,4a-diaza-*s*-indacene (BODIPY) methyl ester has successfully been developed for use as a counterstain for cells and tissues that express green fluorescent protein.[13]

RESULTS AND DISCUSSION

Free base 5,10,15-tris(4-methoxycarbonylphenyl)corrole was prepared according to literature procedures, Scheme 1.[14] Reaction of the free base corrole with PCl_3 in pyridine at 100 °C produces the target molecule **1** in a yield of 92% (for details see Supporting Information). The central atom of **1** was oxidized, P(III) to P(V), due to the ability of porphyrinoids to coordinate O_2 as an axial ligand.[15] The P(III) complex is typically only observed as an intermediate during the phosphorus insertion reaction. The UV−visible absorption spectrum of **1** is similar to those reported previously for transition metal complexes.[6] The MALDI-TOF MS data contain a strong parent peak at m/z 746.23 [calcd $[M + H]^+$ = 746.19], providing direct evidence that the target molecule was obtained. The ^{1}H NMR spectrum of the phosphorus corrole is also typical of a metallocorrolate; the four peaks from 9.47, 9.19, 9.16, and 8.88 ppm are associated with the pyrrole β-protons and were assigned by ^{1}H−^{1}H COSY experiment. The ^{31}P NMR spectrum contains a peak at −100.93 ppm, which is similar to other *meso*-substituted phosphorus(V)-corroles but is significantly different from the peaks reported previously for phosphorus porphyrins, which lie at ca. −200 ppm,[16] due to the complexes being six- rather than five-coordinate.

The optical spectroscopy of corroles can be described in terms of perturbations to an M_L = 0, ±1, ±2, ±3, ±4, ±5, ±6, ±7 sequence of MOs associated with the parent $C_{15}H_{15}^{3-}$ perimeter for the 15-atom 18-π-electron system of the inner ligand perimeter. Moffitt[17] and Michl[18] demonstrated that when the symmetry of aromatic and heteroaromatic π-systems are lowered by perturbations to the structure, the alignments of the nodal patterns of the MOs of the parent perimeter are retained. This can be used to predict the effect of structural perturbations on the relative energies of the frontier π-MOs. The HOMO and LUMO of the parent $C_{15}H_{15}^{3-}$ perimeter for corroles have M_L = ±4 and ±5 properties, respectively. By

dx.doi.org/10.1021/ic402347w | Inorg. Chem. 2014, 53, 2797−2802

Table 1. Calculated Electronic Excitation Spectra of the P(=O) Corrole and P(=O) 5,10,15-Triphenylcorrole Model Complexes and 1 Based on TD-DFT Calculations Using the B3LYP Functional

P(=O) Corrole (C_s)								
band[a]	no.[b]	sym[c]		calc[d]		exp[e]		wave function[f]
	1	$^1A'$						ground state
Q	2	$^1A''$	20.3	492	0.03			60% **s** → −**a**; 39% **a** → −**s**; ...
Q	3	$^1A'$	20.3	491	0.03			61% **a** → −**a**; 39% **s** → −**s**; ...
B	4	$^1A''$	28.1	356	0.61			44% **a** → −**s**; 19% **s** → −**a**; ...
B	5	$^1A'$	28.4	353	0.51			36% **s** → −**s**; 19% 2a″ → −**a**; 15% **a** → −**a**; ...
P(=O) 5,10,15-Triphenylcorrole (C_1)								
band[a]	no.[b]	sym[c]		calc[d]		exp[e]		wave function[f]
	1	^1A						ground state
Q	2	^1A	19.3	518	0.11			65% **s** → −**a**; 33% **a** → −**s**; ...
Q	3	^1A	19.7	507	0.01			58% **a** → −**a**; 43% **s** → −**s**; ...
B	4	^1A	26.6	376	1.06			52% **a** → −**s**; 15% **s** → −**a**; ...
B	5	^1A	26.9	372	0.78			40% **s** → −**s**; 22% **a** → −**a**; ...
1 (C_1)								
band[a]	no.[b]	sym[c]		calc[d]		exp[e]		wave function[f]
	1	^1A						ground state
Q	2	^1A	19.1	524	0.15	16.7	600	65% **s** → −**a**; 32% **a** → −**s**; ...
Q	3	^1A	19.5	514	0.01	17.6	568	57% **a** → −**a**; 42% **s** → −**s**; ...
B	4	^1A	25.3	395	0.65	23.3	429	33% **s** → −**s**; 20% **s** → 4a; 15% **a** → −**a**; ...
B	5	^1A	25.4	394	1.02	24.2	414	43% **a** → −**s**; 20% **s** → 5a; 12% **s** → −**a**; ...

[a]Band assignment described in the text. [b]The number of the state assigned in terms of ascending energy within the TD-DFT calculation. [c]State symmetry. [d]Calculated band energies (10^3 cm^{-1}), wavelengths (nm), and oscillator strengths. [e]Observed energies (10^3 cm^{-1}) and wavelengths (nm). [f]Wave functions based on the eigenvectors predicted by TD-DFT. One-electron transitions associated with the four frontier π-MOs of Michl's perimeter model[14] are highlighted in bold.

analogy with Gouterman's four-orbital model[3] it can be demonstrated that this leads to allowed B and forbidden Q bands based on allowed $\Delta M_L = \pm 1$ and forbidden $\Delta M_L = \pm 9$ transitions. The absorption spectrum of **1** contains bands at 600, 562, and 528 nm in the Q band region and an intense B (or Soret) band at 418 nm, Figure 1. The additional information provided by the MCD technique[19−21] is derived from three highly characteristic spectral features, the Faraday $\mathcal{A}_1$, $\mathcal{B}_0$, and $\mathcal{C}_0$ terms.[18,21−23] The oppositely signed coupled pair of Faraday $\mathcal{B}_0$ terms observed at 600 and 568 nm in the MCD spectrum, Figure 1, can be readily assigned as the Q(0,0) bands, since no other electronic bands are predicted in this portion of the spectrum, Table 1. In the spectra of low-symmetry porphyrinoids, pairs of coupled oppositely signed Faraday $\mathcal{B}_0$ terms replace the derivative-shaped $\mathcal{A}_1$ terms that are observed in the spectra of radially symmetric metal porphyrinoid complexes.[21a]

Michl[18] referred to the two frontier MOs derived from the HOMO and LUMO of the parent perimeter in which nodal planes lie on the *y*-axis as **a** and −**a**, respectively, while the corresponding MOs that lie on antinodes are referred to as **s** and −**s**, Figure 2. In contrast with the analogous porphyrin complex, there is a minor splitting of the −**a** and −**s** MOs of P(=O) corrole for symmetry reasons, due to there being 15 rather than 16 atoms on the perimeter. When phenyl substituents are added at the three *meso*-carbons, there is a narrowing of the HOMO−LUMO gap due to a relative destabilization of the **s** MO, which has large MO coefficients on all three *meso*-carbons, Figures 2 and 3. This leads to a marked red shift of the Q and B bands, Figure 4 and Table 1. There is a further narrowing of the HOMO−LUMO gap when electron-withdrawing −CO_2Me groups are introduced at the *para*-

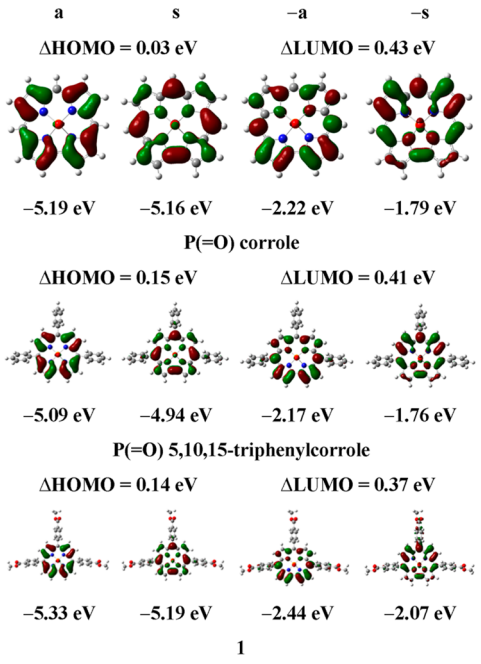

Figure 2. Nodal patterns and energies of the frontier MOs of P(=O) corrole, P(=O) 5,10,15-triphenylcorrole model complexes, and **1** at an isosurface value of 0.03 au. The **a**, **s**, −**a**, and −**s** nomenclature is derived from Michl's perimeter model[18] and refers to four MOs derived from the HOMO and LUMO of a $C_{15}H_{15}^{3-}$ parent hydrocarbon perimeter, based on whether there is a nodal plane or a large MO coefficient on the *meso*-carbon atom which is aligned with the *y*-axis. This nomenclature simplifies the comparison of structurally related molecules of different symmetry.

dx.doi.org/10.1021/ic402347w | Inorg. Chem. 2014, 53, 2797−2802

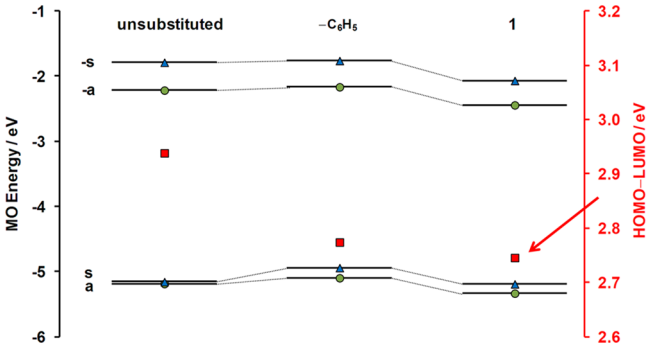

Figure 3. Energies of the frontier π-MOs of the P(=O) corrole and P(=O) 5,10,15-triphenylcorrole model complexes and **1**. The **a**, **s**, **−a**, and **−s** nomenclature is derived from Michl's perimeter model[18] and refers to four MOs derived from the HOMO and LUMO of a $C_{15}H_{15}^{3-}$ parent hydrocarbon perimeter, based on whether there is a nodal plane or a large MO coefficient on the *meso*-carbon atom which is aligned with the *y*-axis. The HOMO−LUMO gap values are plotted against a secondary axis and, as would normally be anticipated, exhibit the same trend that is observed in the calculated energies for the Q and B bands, Figure 4

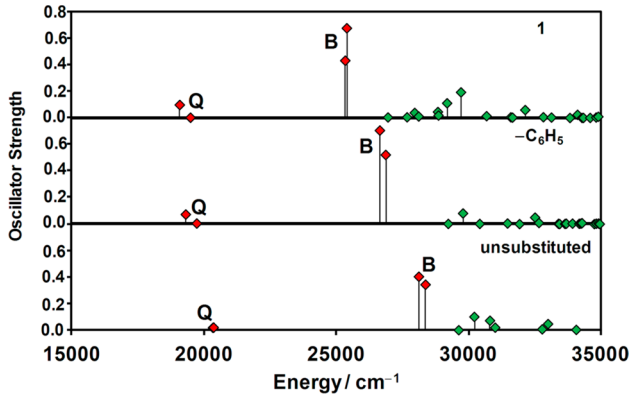

Figure 4. Calculated TD-DFT spectra for the P(=O) corrole and P(=O) 5,10,15-triphenylcorrole model complexes and **1**.

positions of the aryl substituents, due to a relative stabilization of the **−a** and **−s** MOs, Figure 3, which is related to the interaction between the π-systems of the aryl groups and the corrole macrocycle and differences in the size of the MO coefficients on the three *meso*-carbons and at the *para*-positions of the phenyl rings.[18d] This is predicted to cause a further red shift of the Q band toward the biological window for tissue penetration, Figure 4 and Table 1, making the compound more suitable for bioimaging applications. The separation of the MOs derived from the LUMO of the parent perimeter (the ΔLUMO value to use Michl's terminology[18]) is greater than those derived from the HOMO level of the parent perimeter (the ΔHOMO value). This results in an intensification of the Q band of **1** relative to what is observed with analogous porphyrin complexes,[11] due to a mixing of the allowed and forbidden properties of the Q and B bands. Although the Q band remains relatively weak relative to what has been observed in the spectra of the tetraaza analogues of corroles and tetrabenzocorroles[19,20] due to the small |ΔLUMO − ΔHOMO| value,[18] the solubility of the complex is greatly enhanced by the presence of the *meso*-aryl groups, which hinder the aggregation effects due to $\pi-\pi$ stacking that are often observed with phthalocyanine analogues and tend to lead to a quenching of their fluorescence properties.[24]

An intense fluorescence band is observed with a maximum at 610 nm and significant intensity in the 650−700 nm region, Figure 1, and a Stokes shift of 124 cm^{-1} (see Supporting Information). In the absence of a high oxidation state transition metal ion, the lower energy Q(0,0) band of **1** is associated with the S_1 state. The fluorescence quantum value of 0.25 in $CHCl_3$ is similar to that of P(V) tetraphenylporphyrin (Φ_F = 0.28 in ethanol).[12b] The increased intensity of the Q(0,0) bands makes **1** a suitable candidate for use in the imaging of living cells. HeLa cells are the oldest and most commonly used human cell line type in scientific research.[25] HeLa cells were stained with a 10 μM solution of **1** in PBS solution for 10 min at 37 °C and were then studied by confocal fluorescence microscopy (for details see the Supporting Information). Significant intracellular fluorescence was observed, Figure 5. No fluorescence was observed upon irradiation with the lamp of an Olympus FV1000 laser scanning confocal microscope. Only the outlines of the cells are observed in the "bright-field" microscopy images (Figure 5a) since absorbance of incident light identifies dense areas within the sample. Significant intracellular fluorescence was observed upon irradiation with laser light at λ = 543 nm (Figure 5b), however.

Overlays of the fluorescence and bright-field images revealed that this fluorescence signal was selectively located in the

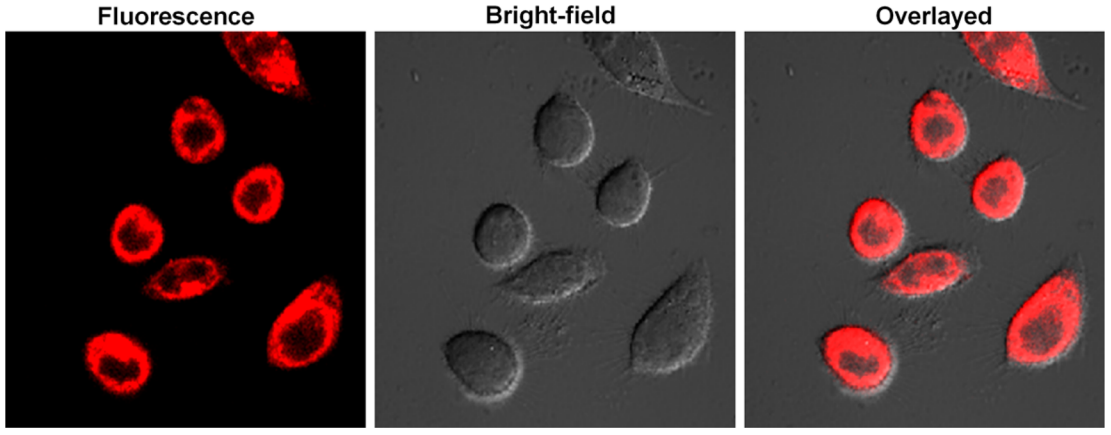

Figure 5. Confocal image luminescence intensity profile (left), the bright-field microscopy image (middle), and overlayed images of HeLa cells incubated with **1** for 10 min at 37 °C with 10 μM in PBS (λ_{ex} = 543 nm).

dx.doi.org/10.1021/ic402347w | Inorg. Chem. 2014, 53, 2797−2802

intracellular region (Figure 5c). The localization of **1** in the nucleus of HeLa cells demonstrates its potential utility for biomaging. More importantly, counterstain results for **1** and 4′,6-diamidino-2-phenylindole (DAPI), Figure 6, demonstrate

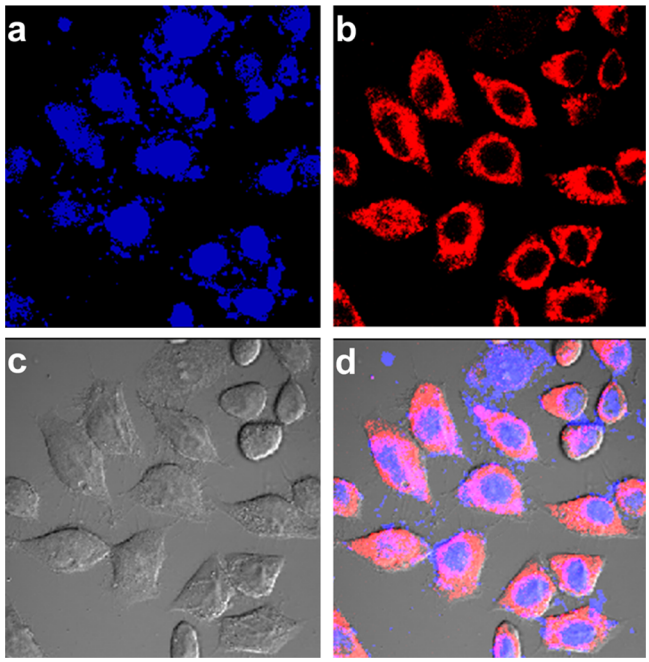

Figure 6. Confocal luminescence imaging of the living HeLa cells. (a) Images of HeLa cells incubated with 0.5 μg/mL DAPI for 5 min at 37 °C (excited at λ = 405 nm). (b) Confocal luminescence images of HeLa cells incubated with compound **1** for 10 min at 37 °C (λ_{ex} = 543 nm). (c) Bright-field images of living HeLa cells. (d) Overlayed luminescence and bright-field pictures.

that the intense fluorescence from the nucleoli and cytoplasm can be easily discriminated from the blue fluorescence in the nuclear zone. This demonstrates that **1** has very good counterstain compatibility with 4′,6-DAPI, which tends to pass through cell membranes, and hence that **1** has good coexistence properties with other types of functional dyes that are used during the bioimaging of living cells. Similar results have recently been reported for a BODIPY methyl ester, which preferentially accumulates in intracellular membranes due to its lipophilic character.[26] Photobleaching studies by laser scanning confocal microscope (LSCM) measurements were also carried out to investigate the photostability of **1** in living cells, Figure 7. The fluorescence signal was detected immediately with no delayed response, and the fluorescence signal is still present after 600 s. Stable output is required for bioimaging agents, so P(V) corroles appear to be potentially useful in this regard. The quantization of the fluorescence intensity profiles of cells stained with **1** is shown in Figure S3.

CONCLUSIONS

The introduction of a P(V) ion into the central cavity of the corrole ligand results in a complex that is potentially suitable for bioimaging applications, since the loss of one of the *meso*-carbons enhances the intensity of the Q band relative to those of tetraphenylporphyrins, and the absence of a high oxidation state transition metal ion results in high Φ_F values. A narrowing of the HOMO−LUMO gap of P(=O) 5,10,15-tris(4-methoxycarbonylphenyl)corrole is predicted relative to that of

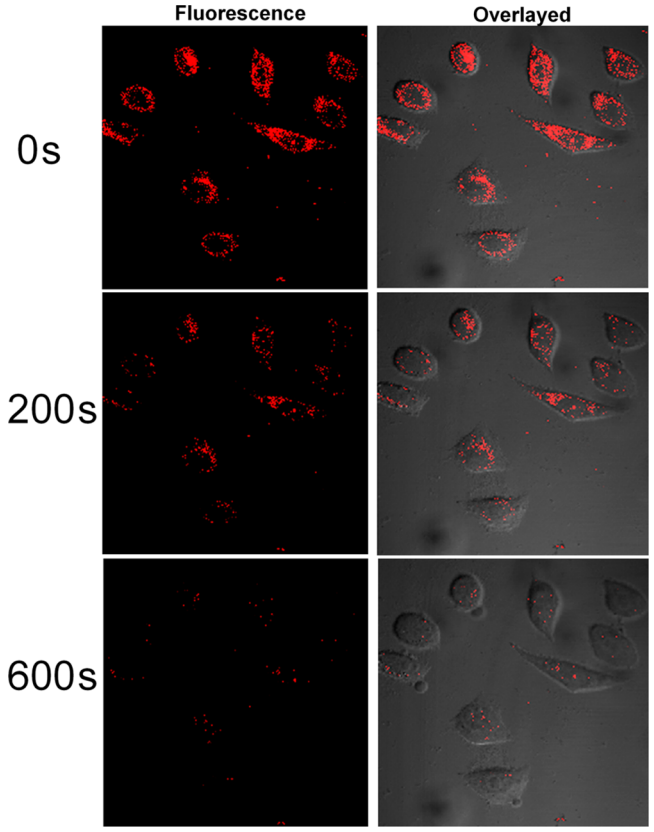

Figure 7. Photobleaching of **1** during LSCM imaging.

the parent corrole ligand, resulting in a red shift of the Q(0,0) bands toward the biological window. There is scope to make further structural modifications, such as fused-ring-expansion of the ligand, to shift the Q bands further to the red through a process of rational design assisted by theoretical calculations. Experiments with HeLa cells demonstrate that P(=O) 5,10,15-tris(4-methoxycarbonylphenyl)corrole is biocompatible and cell-permeable with fluorescence that can be easily discriminated from other types of functional dyes that are used in bioimaging. This suggests that P(V) corroles are potentially useful for applications in this regard and merit further investigation for use in bioimaging.

ASSOCIATED CONTENT

Supporting Information

The experimental details, ^{1}H and ^{31}P NMR spectra, and the quantization of the fluorescence intensity spectra are available free of charge via the Internet at http://pubs.acs.org.

AUTHOR INFORMATION

Corresponding Author

*E-mail: nagaok@m.tohoku.ac.jp. Tel/Fax: +81-22-795-7719.

Notes

The authors declare no competing financial interest.

ACKNOWLEDGMENTS

This work has been supported by Grants-in-Aid for Exploratory Research (No. 25620019) and for Scientific Research Exploratory (B) (No. 23350095) to N.K. from the Ministry of Education, Culture, Sports, Science and Technology, Japan. The theoretical calculations were performed at the Centre for

High Performance Computing in Cape Town, South Africa. We thank Prof. Dr. Fuyou Li (Fudan University, P. R. China) for his help with the living cell bioimaging measurements.

REFERENCES

(1) (a) Kobayashi, N.; Furuyama, T.; Satoh, K. *J. Am. Chem. Soc.* **2011**, *133*, 19642−19645. (b) Isago, H.; Kagaya, Y. *Inorg. Chem.* **2012**, *51*, 8447−8454. (c) Simkhovich, L.; Mahammed, A.; Goldberg, I.; Gross, Z. *Chem.—Eur. J.* **2001**, *7*, 1041−1055.

(2) (a) Escobedo, J. O.; Rusin, O.; Lim, S.; Strongin, R. M. *Curr. Opin. Chem. Biol.* **2010**, *14*, 64. (b) Ethirajan, M.; Chen, Y.; Joshi, P.; Pandey, R. K. *Chem. Soc. Rev.* **2011**, *40*, 340−362. (c) Kuimova, M. K.; Collins, H. A.; Balaz, M.; Dahlstedt, E.; Levitt, J. A.; Sergent, N.; Suhling, K.; Drobizhev, M.; Makarov, N. S.; Rebane, A.; Anderson, H. L.; Phillips, D. *Org. Biomol. Chem.* **2009**, *7*, 889−896. (d) Zhang, J.-X.; Zhou, J.-W.; Chan, C.-F.; Lau, T. C.-K.; Kwong, D. W. J.; Tam, H.-L.; Mak, N.-K.; Wong, K.-L.; Wong, W.-K. *Bioconjugate Chem.* **2012**, *23*, 1623−1638. (e) Kitagishi, H.; Hatada, S.; Itakura, T.; Maki, Y.; Maeda, Y.; Kano, K. *Org. Biomol. Chem.* **2013**, *11*, 3203−3211. (f) Karunakaran, S. C.; Babu, P. S. S.; Madhuri, B.; Marydasan, B.; Paul, A. K.; Nair, A. S.; Rao, K. S.; Srinivasan, A.; Chandrashekar, T. K.; Rao, Ch. M.; Pillai, R.; Ramaiah, D. *ACS Chem. Biol.* **2013**, *8*, 127−132. (g) Zhao, Q.; Huang, C.; Li, F. *Chem. Soc. Rev.* **2011**, *40*, 2508−2524.

(3) Gouterman, M. In *The Porphyrins*; Dolphin, D., Ed.; Academic Press: New York, 1978; Vol. *III*, Part A, pp 1−165.

(4) (a) Akers, W.; Lesage, F.; Holten, D.; Achilefu, S. *Mol. Imaging* **2007**, *6*, 237−246. (b) Pandey, R. K.; Goswami, L. N.; Chen, Y.; Gryshuk, A.; Missert, J. R.; A. Oseroff, A.; Dougherty, T. J. *Lasers Surg. Med.* **2006**, *38*, 445−467. (c) Kee, H. L.; Nothdurft, R.; Muthiah, C.; Diers, J. R.; Fan, D.; Ptaszek, M.; Bocian, D. F.; Lindsey, J. S.; Culver, J. P.; Holten, D. *Photochem. Photobiol.* **2008**, *84*, 1061−1072.

(5) (a) Erben, C.; Will, S.; Kadish, K. M. In *The Porphyrin Handbook*, Vol. 2; Kadish, K. M.; Smith, K. M.; Guilard, R., Eds.; Academic Press, Inc.: London, 2000; pp 232−300. (b) Guilard, R.; Barbe, J.-M.; Stern, C.; Kadish, K. M. In *The Porphyrin Handbook*, Vol. *18*; Kadish, K. M.; Smith, K. M.; Guilard, R., Eds.; Academic Press, Inc.: London, 2003; pp 303−351.

(6) (a) Paolesse, R. In *The Porphyrin Handbook*, Vol. 2; Kadish, K. M.; Smith, K. M.; Guilard, R., Eds.; Academic Press, Inc.: London, 2000; pp 201−231. (b) Goldberg, D. P. *Acc. Chem. Res.* **2007**, *40*, 626−634.

(7) Simkhovich, L.; Mahammed, A.; Goldberg, I.; Gross, Z. *Chem.—Eur. J.* **2001**, *7*, 1041−1055.

(8) (a) Agadjanian, H.; Weaver, J. J.; Mahammed, A.; Rentsendorj, A.; Bass, S.; Kim, J.; Dmochowski, I. J.; Margalit, R.; Gray, H. B.; Gross, Z.; Medina-Kauwe, L. K. *Pharm. Res.* **2006**, *23*, 367−377. (b) Agadjanian, H.; Ma, J.; Rentsendorj, A.; Valluripalli, V.; Hwang, J. Y.; Mahammed, A.; Farkas, D. L.; Gray, H. B.; Gross, Z.; Medina-Kauwe, L. K. *Proc. Natl. Acad. Sci. U.S.A.* **2009**, *106*, 6105−6110. (c) Hwang, J. Y.; Lubow, J.; Chu, D.; Ma, J.; Agadjanian, H.; Sims, J.; Gray, H. B.; Gross, Z.; Farkas, D. L.; Medina-Kauwe, L. K. *Mol. Pharmaceutics* **2011**, *8*, 2233−2243. (d) Lim, P.; Mahammed, A.; Okun, Z.; Saltsman, I.; Gross, Z.; Gray, H. B.; Termini, J. *Chem. Res. Toxicol.* **2012**, *25*, 400−409. (e) Hwang, J. Y.; Lubow, D. J.; Sims, J. D.; Gray, H. B.; Mahammed, A.; Gross, Z.; Medina-Kauwe, L. K.; Farkas, D. L. *J. Biomed. Opt.* **2012**, *17*, 015003.

(9) (a) Aviv-Harel, I.; Zeev Gross, Z. *Coord. Chem. Rev.* **2011**, *255*, 717−736. (b) Albrett, A. M.; Boyd, P. W.; Clark, G. R.; Gonzalez, E.; Ghosh, A.; Brothers, P. J. *Dalton Trans.* **2010**, *39*, 4032−4034. (c) Albrett, A. M.; Conradie, J.; Ghosh, A.; Brothers, P. J. *Dalton Trans.* **2008**, *33*, 4464−4473.

(10) (a) Paolesse, R.; Boschi, T.; Licoccia, S.; Khoury, R. G.; Smith, K. M. *Chem. Commun.* **1998**, 1119−1120. (b) Kadish, K. M.; Ou, Z. P.; Adamian, V. A.; Guilard, R.; Gros, C. P.; Erben, C.; Will, S.; Vogel, E. *Inorg. Chem.* **2000**, *39*, 5675−5682.

(11) (a) Sayer, P.; Gouterman, M.; Connell, C. R. *J. Am. Chem. Soc.* **1977**, *99*, 1082−1087. (b) Carrano, C. J.; Tsutsui, M. J. *Coord. Chem.* **1977**, *7*, 79−83. (c) Mangani, S.; Meyer, E. F.; Cullen, D. L.; Tsutsui, M.; Carrano, C. J. *Inorg. Chem.* **1983**, *22*, 1858−1862. (d) Andou, Y.; Ishikawa, K.; Shima, K.; Shiragami, T.; Yasuda, M. *Bull. Chem. Soc. Jpn.* **2002**, *75*, 1757−1760.

(12) (a) Hirakawa, K.; Kawanishi, S.; Matsumoto, J.; Shiragami, T.; Yasuda, M. *J. Photochem. Photobiol. B* **2006**, *82*, 37−44. (b) Hirakawa, K.; Kawanishi, S.; Hirano, T.; Segawa, T. *J. Photochem. Photobiol. B* **2007**, *87*, 209−217.

(13) (a) Godinho, L.; Mumm, J. S.; Williams, P. R.; Schroeter, E. H.; Koerber, A.; Park, S. W.; Leach, S. D.; Wong, R. O. *Development* **2005**, *132*, 5069−5079. (b) Cooper, M. S.; Szeto, D. P.; Sommers-Herivel, G.; Topczewski, J.; Solnica-Krezel, L.; Kang, H. C.; Johnson, I.; Kimelman, D. *Dev. Dyn.* **2005**, *232*, 359−368. (c) Goodin, M.; Yelton, S.; Ghosh, D.; Mathews, S.; Lesnaw, J. *Mol. Plant-Microbe Interact.* **2005**, *18*, 703−709. (d) Jensen, P. J.; Gitlin, J. D.; Carayannopoulos, M. O. *J. Biol. Chem.* **2006**, *281*, 13382−13387. (e) Bendezú, F. O.; de Boer, P. A. *J. Bacteriol.* **2008**, *190*, 1792−1811. (f) Reddy, K. L.; Zullo, J. M.; Bertolino, E.; Singh, H. *Nature* **2008**, *452*, 243−247. (g) Kim, M.; Bellini, M.; Ceman, S. *Mol. Cell. Biol.* **2009**, *29*, 214−228.

(14) Gryko, D. T.; Koszarna, B. *Org. Biomol. Chem.* **2003**, *1*, 350−357.

(15) (a) Sayer, P.; Gouterman, M.; Connell, C. R. *J. Am. Chem. Soc.* **1977**, *99*, 1082−1087. (b) Carrano, C. J.; Tsutsui, M. *J. Coord. Chem.* **1977**, *7*, 79−83. (c) Mangani, S.; Meyer, E. F.; Cullen, D. L.; Tsutsui, M.; Carrano, C. J. *Inorg. Chem.* **1983**, *22*, 1858−1862.

(16) Barbour, T.; Belcher, W. J.; Brothers, P. J.; Rickard, C. E. F.; Ware, D. C. *Inorg. Chem.* **1992**, *31*, 746−754.

(17) (a) Moffitt, W. J. *Chem. Phys.* **1954**, *22*, 320−333. (b) Moffitt, W. J. *Chem. Phys.* **1954**, *22*, 1820−1829.

(18) (a) Michl, J. *J. Am. Chem. Soc.* **1978**, *100*, 6801−6811. (b) Michl, J. *J. Am. Chem. Soc.* **1978**, *100*, 6812−6818. (c) Michl, J. *Pure Appl. Chem.* **1980**, *52*, 1549−1570. (d) Michl, J. *Tetrahedron* **1984**, *40*, 3845−3934.

(19) Mack, J.; Bunya, M.; Lansky, D.; Goldberg, D. P.; Kobayashi, N. *Heterocycles* **2008**, *76*, 1369−1380.

(20) Mack, J.; Kobayashi, N. *Chem. Rev.* **2011**, *111*, 281−321.

(21) (a) Mack, J.; Stillman, M. J.; Kobayashi, N. *Coord. Chem. Rev.* **2007**, *251*, 429−453. (b) Kobayashi, N.; Muranaka, A.; Mack, J. *Circular Dichroism and Magnetic Circular Dichroism Spectroscopy for Organic Chemists*; Royal Society of Chemistry: Cambridge, 2011.

(22) Piepho, S. B.; Schatz, P. N. *Group Theory in Spectroscopy with Applications to Magnetic Circular Dichroism*; John Wiley and Sons: New York, 1983.

(23) Stephens, P. J. *Adv. Chem. Phys.* **1976**, *35*, 197−264.

(24) (a) Dhami, S.; De Mello, A. J.; Rumbles, G.; Bishop, S. M.; Phillips, D.; Beeby, A. *Photochem. Photobiol.* **1995**, *61*, 341−346. (b) Petrášeka, Z.; Phillips, D. *Photochem. Photobiol. Sci.* **2003**, *2*, 236−244.

(25) (a) William, F.; Scherer, J. T.; George, O. G. *J. Exp. Med.* **1997**, *5*, 695−710. (b) Davis, A. C.; Theodosopoulos, G.; Atkin, A.; Drexler, H. G.; Kohara, A.; MacLeod, R. A. F.; Masters, J. R.; Nakamura, Y.; Reid, Y. A.; Reddel, R. R.; Freshney, R. L. *Int. J. Cancer* **2010**, *127*, 1−8.

(26) (a) Zhang, P.; Hu, L.; Yin, Q.; Feng, L.; Li, Y. *Mol. Pharmaceutics* **2012**, *9*, 1590−1598. (b) Heek, T.; Nikolaus, J.; Schwarzer, R.; Fasting, C.; Welker, P.; Licha, K.; Herrmann, A.; Haag, R. *Bioconjugate Chem.* **2013**, *24*, 153−158.